

# Universal behavior in the static and dynamic properties of the $\alpha$ -XY model

Andrea Giansanti<sup>a,§</sup>, Daniele Moroni<sup>a,†</sup> and Alessandro Campa<sup>b,‡</sup>

<sup>a</sup>Dipartimento di Fisica, Università di Roma “La Sapienza” and INFN Unità di Roma1,  
Piazzale Aldo Moro 2, 00185 Roma, Italy

<sup>b</sup>Laboratorio di Fisica, Istituto Superiore di Sanità and INFN Sezione di Roma1, Gruppo Collegato Sanità  
Viale Regina Elena 299, 00161 Roma, Italy

(8<sup>th</sup> November 2000)

Accepted for publication in Chaos Solitons and Fractals:  
Special issue. Proceedings of the International Workshop:  
*Classical and Quantum Complexity and Nonextensive Thermodynamics*,  
Denton (Texas), April 3-6 2000.

## Abstract

The  $\alpha$ -XY model generalizes, through the introduction of a power-law decaying potential, a well studied mean-field hamiltonian model with attractive long-range interactions. In the  $\alpha$ -model, the interaction between classical rotators on a lattice is gauged by the exponent  $\alpha$  in the couplings decaying as  $r^\alpha$ , where  $r$  are distances between sites. We review and comment here a few recent results on the static and dynamic properties of the  $\alpha$ -model. We discuss the appropriate  $\alpha$  dependent rescalings that map the canonical thermodynamics of the  $\alpha$ -model into that of the mean field model. We also show that the chaotic properties of the model, studied as a function of  $\alpha$  display a universal behaviour.

<sup>§</sup>Corresponding author; Andrea.Giansanti@roma1.infn.it

<sup>‡</sup>Campa@iss.infn.it

<sup>†</sup>smoroni@lucifero.phys.uniroma1.it

# 1 Introduction

Equilibrium Classical Statistical Mechanics is one of the grounds of modern physics; it originated from the works of Boltzmann and Gibbs at the end of 19th century. The computational techniques of Statistical Mechanics, generalized to encompass the right enumeration of quantum states, have been successfully applied to the study of all states of matter, along all the 20th century. On one side, the rigorous analysis of this branch of theoretical physics has been impressive and far reaching [1][2] and the belief that everything in this field has been robustly founded seems to be quite widespread. On the other side there has been a serendipitous pragmatic use of the Boltzmann-Gibbs approach beyond the bounds set by theorems. The use of Equilibrium Statistical Mechanics outside the allowed boundaries led to the discovery of anomalies or paradoxes, particularly in the field of self-gravitating systems[3][4]. In fact all the edifice of statistical mechanics rests on few stringent assumptions on the interactions that are not fulfilled by long-range forces. In spite of their fundamental relevance, gravitational and Coulombic forces do not fit in with Equilibrium Classical Statistical Mechanics[5].

Short-range interactions guarantee extensivity: that is energy and entropy, as functions of intensive internal parameters, grow linearly with the number  $N$  of microscopic components of the systems. If an extensive system is divided into macroscopic parts the total energy and entropy is the sum of the energies and entropies of the parts. On the contrary that is not true in systems where long-range interactions can reflect themselves in thermodynamic potentials that do not scale with the size of the system and cannot be defined in the thermodynamic limit (i. e. for  $N$  going to infinity). Moreover, long-range forces may well induce strong spatial and temporal dynamic correlations that contrast mixing and result either in very long relaxation times or in equilibrium distributions different from the expected Boltzmann-Gibbs.

Aiming at a microscopic foundation of non extensive thermodynamics a good starting point is the study of the ergodic properties in the thermodynamic limit of simple and meaningful Hamiltonian models with long-range interactions [6]. In the recent past Stefano Ruffo and co-workers have introduced a class of mean-field models with infinite range of the interactions [7]. These models are related with the statistical physics of self-gravitating systems and that of phase transitions and became paradigmatic in the study of non-extensivity. In particular, the dynamics and thermodynamics of the so called Hamiltonian Mean-Field model (HMF) have been extensively studied in the last few years and a comprehensive review can be found in the contribution to these proceedings by Andrea Rapisarda and Vito Latora [8].

The  $\alpha$ -XY model we refer to in this paper has been introduced by Celia Anteneodo and Constantino Tsallis [9]; this model cleverly combines the physics of the mean-field models quoted above with the statistical physics of lattice models of the Ising type with long-range couplings decaying as the inverse power  $\alpha$  of the distances between sites. Since classical works on the foundations of Statistical Mechanics [10] it has been known that these systems are non extensive for  $0 \leq \alpha/d < 1$ , where  $d$  is the dimensionality of the ambient space;  $\alpha/d$  is then the natural control parameter of non extensivity in this class of models.

Our work originated from previous works by other researchers active in the fields: in the section devoted to the thermodynamics of the  $\alpha$ -XY model a

canonical solution is presented that has been largely inspired by the analytical work of Antoni and Ruffo on the HMF model [11] and by a numerical work by Tamarit and Anteneodo [12] [13]; in the section about dynamics the results on the Lyapunov exponents extend the previous work by Anteneodo and Tsallis [9]. In the conclusions we try to express our point of view about the connection of our results with the particular form of nonextensive thermodynamics proposed by Tsallis [14].

## 2 Thermodynamics

In this section we define the model and we compute its canonical partition function. We use the typical methods of Gaussian transformation and saddle point integration together with a Fourier diagonalization of the interaction potential.

### 2.1 Definition of the model

We consider the hamiltonian of a system of bidimensional classical rotators (XY spins):

$$H = K + V = \frac{1}{2} \sum_{i=1}^N L_i^2 + \frac{1}{2\tilde{N}} \sum_{i \neq j}^N \frac{1 - \cos(\theta_i - \theta_j)}{r_{ij}^\alpha}. \quad (1)$$

The  $N$  spins are placed at the sites of a generic  $d$ -dimensional lattice, and each one is represented by the conjugate canonical pair  $(L_i, \theta_i)$ , where the  $L_i$ 's are the angular momenta (unit momentum of inertia is assumed) and the  $\theta_i$ 's  $\in [0, 2\pi)$  are the angles of rotation on a family of parallel planes, each one defined at each lattice point. The interaction between rotators  $i$  and  $j$  decays as the inverse of their distance  $r_{ij}$  to the power  $\alpha \geq 0$ . Periodic boundary conditions are assumed in the form of nearest image convention.

The hamiltonian is extensive if the thermodynamic limit (TL)  $N \rightarrow \infty$  of the canonical partition function  $(\ln Z)/N$  exists and is finite. This is assured for each  $\alpha$  by the presence of the rescaling factor  $\tilde{N}$  in front of the double sum of the potential energy.  $\tilde{N}$  is a function of the lattice parameters  $\alpha, d, N$  which is proportional to the range  $S$  of the interaction defined by:

$$\tilde{N} \propto S = \sum_{j \neq i} \frac{1}{r_{ij}^\alpha}. \quad (2)$$

The sum is independent of the origin  $i$  because of periodic conditions. Then, for each  $\alpha$ ,  $V$  is proportional to  $N$ . When  $\alpha > d$ , which we call here the *short-range* case,  $S$  is finite in the TL [15], and things go as if each rotator interacted with a finite number of rotators, those within range  $S$ . On the contrary when  $\alpha < d$ , which we consequently call the *long-range* case,  $S$  diverges in the TL and the factor  $1/\tilde{N}$  in (1) compensates for this.

The model (1) is intimately connected to its mean-field version for  $\alpha = 0$ , introduced by Antoni and Ruffo in [11] and called HMF model:

$$H = \frac{1}{2} \sum_{i=1}^N L_i^2 + \frac{1}{2N} \sum_{i,j=1}^N [1 - \cos(\theta_i - \theta_j)]. \quad (3)$$

The model is a classical ferromagnetic XY model and undergoes a ferromagnetic transition from a high temperature paramagnetic state crossing the critical temperature  $T_c = 1/2$  corresponding to a critical energy  $U_c = 3/4$ . The computation of the partition function of the full  $\alpha$  model, eq. (1) is a straightforward generalization of the procedure followed for the HMF model, using the standard methods of Gaussian transformation and saddle point technique, the whole treatment being successful only for the long-range case  $\alpha < d$ . We resume here the main passages, whereas a more detailed explanation can be found in [16].

## 2.2 Partition function

The partition function of model (1) factorizes in a trivial kinetic contribution  $Z_K = (2\pi/\beta)^{N/2}$  and a nontrivial potential part

$$Z_V = \int_{-\pi}^{\pi} d^N \theta \exp(-\beta V), \quad (4)$$

where  $\beta = 1/(\kappa_B T)$  is the inverse temperature. We rewrite the potential part as

$$V = \frac{1}{2\tilde{N}} \sum_{i \neq j}^N \frac{1 - \cos(\theta_i - \theta_j)}{r_{ij}^\alpha} - \mathbf{h} \cdot \sum_{i=1}^N \mathbf{m}_i \quad (5)$$

where we have introduced an external field  $\mathbf{h} = (h_x, h_y)$  and defined a local magnetization vector  $\mathbf{m}_i = (m_{ix}, m_{iy}) = (\cos \theta_i, \sin \theta_i)$ . The total magnetization is then given by  $\mathbf{M} = (M_x, M_y) = \frac{1}{N} \sum_{i=1}^N \mathbf{m}_i$ . The integral (4) is remanipulated introducing matrix conventions. The constraint  $i \neq j$  over the double sum is removed defining  $r_{ii}^\alpha = 1/b$ , a finite number. Since the numerator  $1 - \cos(\theta_i - \theta_j)$  is zero for  $i = j$  the choice of  $b$  is free. The removal of the constraint allows us to introduce the distance matrix  $R_{ij} = \beta/(2\tilde{N}r_{ij}^\alpha)$ . After defining  $\mathbf{B} = \beta\mathbf{h}$  and  $C = \exp[-\beta/(2\tilde{N}) \sum_{ij} (1/r_{ij}^\alpha)]$ , the potential part can be written as:

$$Z_V = C \int_{-\pi}^{\pi} d^N \theta \exp \left[ \sum_{i,j,\mu} m_{i\mu} R_{ij} m_{j\mu} + \sum_i B_\mu m_{i\mu} \right], \quad (6)$$

where  $\mu = x, y$ . Diagonalizing the distance matrix  $R = (R_{ij})$  we can write the first part of the exponent in (6) in a suitable form for application of gaussian transformation. The formula requires real and positive eigenvalues: the first condition is satisfied because the matrix is symmetric and the second by a proper choice of parameter  $b$  because, as it can be easily seen, the entire spectrum is linearly translated by it.

Application of the formula leads to known integrals in variables  $\theta_i$  and the whole  $Z_V$  can be rewritten as

$$Z_V = C \frac{\det R}{\pi^N} \int_{-\infty}^{+\infty} d^N \Psi_x d^N \Psi_y \quad (7)$$

$$e^{N \left[ - \sum_{i,j,\mu} \Psi_{i\mu} \frac{R_{ij}}{N} \Psi_{j\mu} + \frac{1}{N} \sum_i \ln \left( 2\pi I_0 \left( |2 \sum_j R_{ij} \Psi_j + \mathbf{B}| \right) \right) \right]},$$

where  $I_0$  is the zeroth-order modified Bessel function and the  $\Psi_i$ 's are the gaussian variables. Use of the saddle point technique is now more delicate than in

the mean-field case and requires a careful study of the first and second derivative of the function in square brackets at the exponential in eq. (7), which we call  $f(w)$ , where  $w = (\Psi_{1x}, \dots, \Psi_{Nx}, \Psi_{1y}, \dots, \Psi_{Ny})$ . The maximum is obtained for a vector  $w_0 = (\Psi_x, \dots, \Psi_x, \Psi_y, \dots, \Psi_y)$ , homogeneous on the lattice sites. Defining  $\Psi = (\Psi_x, \Psi_y)$ , its direction is that of  $\mathbf{B}$ , and its modulus  $\Psi$  is given by the solution of the self-consistency equation:

$$\Psi = \frac{I_1}{I_0} (\beta [A\Psi + h]) , \quad (8)$$

with

$$A = \frac{1}{\bar{N}}[b + S] = \frac{1}{\bar{N}} \left[ b + \sum_{j \neq i} \frac{1}{r_{ij}^\alpha} \right] , \quad (9)$$

and where  $I_1$  is the first order modified Bessel function. We note that when  $h = 0$  we have infinitely many degenerate solutions, since only the modulus  $\Psi$  is determined.

Evaluation of the elements of the hessian matrix of  $f(w)$  at the stationary point just proves that it is a maximum. Full application of the saddle-point method gives the potential energy contribution to the free energy per particle  $-\beta F$  in the TL as  $f(w_0)$  plus a second-order correction which can be estimated as

$$\lim_{N \rightarrow \infty} \frac{1}{N} \sum_{\mathbf{k}} \ln[1 - (\dots) R_{\mathbf{k}}] , \quad (10)$$

where  $R_{\mathbf{k}}$  are the eigenvalues of matrix  $R$ . Because of translational invariance (in turn due to periodic conditions) they can be computed through Fourier transform and thus labelled by the reciprocal lattice vectors  $\mathbf{k}$ . The  $N$  rescaling involved in the definition of the matrix  $R$  is the key feature to estimate the correction. When  $\alpha < d$  it is found that most of the eigenvalues go to zero in the TL, the quantity being given by  $N'$  such that  $N'/N \rightarrow 0$ . The same estimate then applies to eq. (10) and the second-order correction effectively vanishes. The procedure cannot be extended to  $\alpha > d$  because no divergence occurs in the spectrum.

Once obtained the free energy, differentiation with respect to thermodynamic variables gives the total magnetization  $M$ , which is found to coincide with the gaussian variable  $\mathbf{M} = \Psi$ , and the internal energy

$$U = \frac{1}{2\beta} + \frac{A}{2}(1 - M^2) - hM . \quad (11)$$

### 2.3 Universality

Equations (8) and (11) have the exact form of the mean field equations as soon as one takes  $A = 1$  or, otherwise stated, as soon as the proportionality in eq. (2) is replaced by an equality. As we show below with this position in the long-range case the partition function of the model then completely reduces to that of the mean-field case and with it the equations of state, namely the magnetization curve  $M$  vs  $U$ , and the caloric curve  $T$  vs  $U$  where the internal energy is  $U = \langle H/N \rangle$ . The thermodynamic of the model thus becomes *universal* in the sense of being independent of the value of  $\alpha, d$  for any  $\alpha < d$ .

As a consequence it shows a ferromagnetic transition at the universal critical mean field energy  $U_c = 3/4$ . There is a slight difference between an equality in eq. (2) and the position  $A = 1$ , caused by the term  $b$  in eq. (9) but it loses significance in the TL because of the divergence of the second term in  $S$ . For finite  $N$  it is a simple matter of computation that the right definition to obtain universal state curves is really

$$\tilde{N} = S = \sum_{j \neq i} \frac{1}{r_{ij}^\alpha}. \quad (12)$$

Indeed physical equations cannot depend on a pure mathematical parameter, such as  $b$ . Take for example the high energy form of the caloric equation of state. Because the term  $\cos(\theta_i - \theta_j)$  in eq. (1) is null on average (each rotator being approximately free), using equipartition of energy we find  $2U \sim T + S/\tilde{N}$ . In order to numerically obtain a universal equation of state we must make this expression coincide with the HMF one  $2U \sim T + 1$  and equation (12) is required.

Then we have shown that any model with  $\alpha < d$  on any lattice is equivalent to HMF if we assume eq. (12). The theoretical computation supports the simulative results found in [12] for a onedimensional lattice. As a further check of the theoretical result we simulated the system on a simple cubic three-dimensional lattice through constant energy molecular dynamics applied to hamiltonian (1). We used a fourth-order symplectic algorithm [17] with time step 0.02, selected to have relative energy fluctuations not exceeding  $1/10^6$ . We have chosen a fixed  $N = 343 = 7^3$ , and have simulated various energy densities  $H/N$  and various  $\alpha < 3$ . In Fig. 1 we show that the numerical caloric curves collapse onto the universal HMF curve and in Fig. 2 we show the same for the magnetization curve. In the same figures we report simulations for one value of  $\alpha > d$  to stress the impossibility to extend the previous treatment to the short-range case. The curves are qualitatively different: the caloric one has an everywhere continuous derivative and lacks the finite discontinuity at the critical energy, and the magnetization curve has a different critical exponent. As the inset shows if one tries to rescale the abscissa for the  $\alpha > d$  magnetization curve in order to let it coincide with the mean field one, a fundamentally different behaviour appears. As known from renormalization group studies in fact the critical exponent for the first-neighbour ( $\alpha = \infty$ ) model is  $\sim 0.36$  [18] different from the mean-field value 0.5.

It is also interesting to observe the extrapolation which follows from eq. (12). If one estimates from this equation a *mean* value for  $1/r_{ij}^\alpha$  one immediately finds  $1/r_{ij}^\alpha \sim \tilde{N}/N$ . Insertion of this esteem into equation (1) directly provides the fundamental HMF hamiltonian, eq. (3). This remark naturally supports the previous analytical work, however we point out that it cannot fully justify it because it leads to a wrong conclusion in the short-range case  $\alpha > d$ .

The physical reason for universality can be given considering a single rotator surrounded by all others. It effectively interacts only with the rotators within range  $S$  (interaction area). For fixed  $N$  and varying  $\alpha$  this area goes from all the lattice for  $\alpha = 0$  to the only first neighbours for  $\alpha = \infty$ . Increasing  $N$ , if  $\alpha < d$  the range  $S$  diverges and the interaction area expands as well, while if  $\alpha > d$  the range stays finite and the area localized. The idea is shown in Fig. 3. When  $N \rightarrow \infty$  all interaction areas for  $\alpha < d$  simply become all the space, in the same way it occurs at finite  $N$  only for  $\alpha = 0$ . The way the interaction areas

diverge obviously depends on  $\alpha$  (see note [15]) but once at the infinity it does not matter how you got there. All interaction areas are infinite and equal to each other. Simply adapting the interaction field through rescaling you obtain that each rotator feels all the others with the same strength, independently of  $\alpha, d$ .

This reasoning cannot be extended to the case  $\alpha > d$ . Even for  $N$  going to infinity the interaction area remains a well defined localized zone, its features depending on  $\alpha$  and the conformation of the neighbourhood.

### 3 Dynamics

#### 3.1 Lyapunov exponents in the thermodynamic limit

We study the maximal Lyapunov exponent, as defined by the limit [19]:

$$\lambda_{max} = \lim_{t \rightarrow \infty} \frac{1}{t} \ln \frac{d(t)}{d(0)} = \lim_{t \rightarrow \infty} \lambda(t), \quad (13)$$

with  $d(t) = \sqrt{\sum_i (\delta\theta_i)^2 + (\delta L_i)^2}$  being the metric distance calculated from infinitesimal displacements at time  $t$  obtained in turn through the double integration of both the normal equations of motion

$$\dot{\theta}_i = L_i \quad (14)$$

$$\dot{L}_i = \sum_{j \neq i} \frac{\sin(\theta_j - \theta_i)}{\tilde{N} r_{ij}^\alpha} \quad (15)$$

and the linearized ones

$$\delta\dot{\theta}_i = \delta L_i \quad (16)$$

$$\delta\dot{L}_i = \sum_{j \neq i} \frac{\cos(\theta_j - \theta_i)}{\tilde{N} r_{ij}^\alpha} (\delta\theta_j - \delta\theta_i), \quad (17)$$

as obtained from hamiltonian (1). In the same simulations of the previous section we also computed  $\lambda_{max}$  constructing the curves  $\lambda_{max}(U)$  for various value of  $\alpha$ . We report the results in Fig. 4.

We note a common behaviour for all the curves at  $\alpha < d$ . Though not perfectly coincident they all show a definite peak around the critical energy  $U_c = 0.75$ , resembling the HMF behaviour as found for example in [20][21][22][23][24]. On the contrary the curve for  $\alpha/d = 5$  is different. Besides having a highest maximum, it clearly lacks a well defined peak, and it much more resembles the first-neighbour behaviour [25][26].

We also investigated how  $\lambda_{max}$  for varying  $\alpha/d$  from 0 to  $\infty$  goes from the HMF-like behaviour to the other one typical of the first-neighbour model.

We simulated the system at fixed energy density  $U_c = 0.6$ , varying  $\alpha/d$  and for  $N = 343$  and  $N = 125$ . The results are shown in Fig. 5. In accordance with Fig. 4 the points for  $\alpha < d$  are much closer to each other, the vicinity increasing for higher  $N$ . In the curve for  $N = 125$  a smooth ascent for low  $\alpha/d$  suddenly increases after  $\alpha/d = 0.5$ . The curve for  $N = 343$ , though showing a similar behaviour, presents the increase for  $\alpha/d = 0.75$ . We conjecture that for

still higher  $N$  the point of sharp increase moves towards  $\alpha/d = 1$  and then in the TL we have

$$\lambda_{max}(\alpha, d) = \lambda_{max}(\alpha = 0) \quad \forall \alpha < d. \quad (18)$$

We checked this conjecture with a more careful study for fixed high energy  $U = 5.0 > U_c$ . The complete details can be found in [27]. These simulations were done using a velocity-Verlet [28] algorithm with a time-step chosen to have a relative energy conservation of  $10^{-4}$  or better. Length of simulations were chosen looking at the asymptotic behavior of quantity  $\lambda(t)$ , eq. (13), where  $d(0)$  is randomly chosen (see [19]). We report in Fig. 6, the curves  $\lambda_{max}(N)$  for various  $\alpha$  in dimensions  $d = 3$ .

Because for the HMF model has been theoretically [24] and simulatively found that  $\lambda_{max}(U > U_c, N \rightarrow \infty) = 0$ , it is clearly seen that eq. (18) is satisfied. We observe that, for growing  $N$ , if  $\alpha > d$  then  $\lambda_{max}$  is positive and constant, whereas if  $\alpha < d$  the maximal Lyapunov exponent tends to zero, the value of HMF model. The same behaviour has been found in dimension  $d = 1$  [9] and  $d = 2$  [27].

Then we can believe that in the TL the behaviour of the maximal Lyapunov exponent is universal, its dependence on the energy density  $U$  being the same universal curve which can be found in Fig. 2 of [24].

### 3.2 Finite $N$ case

We have also investigated the scaling law for the reduction with  $N$  of the Maximal Lyapunov Exponents. We report here the results shown in [27].

For any finite  $N$  we have fitted the data with the following functional form:  $\lambda_{max} \propto N^{-\kappa}$ ;  $\kappa$  being the slope in the log-log plots of Fig. 6. Collecting the slopes  $\kappa$  as a function of the ratio  $\alpha/d$ , for  $d = 1, 2, 3$ , remarkably, through the simple scaling  $\alpha/d$ , the  $N$  dependence of the maximal Lyapunov exponent of model (1) is universal. All curves start at  $\alpha = 0$  from a value close to  $1/3$ , analytically and numerically found for the HMF model [21][24]; when  $\alpha/d$  increases from zero to unity all our data collapse into a single curve, and then remain zero for  $\alpha/d$  greater than unity. And the universal function  $\kappa$ , shown in Fig. 7, does not appear to depend on the energy density, provided this is greater than the critical one.

## 4 Quasi Stationary States

In literature there is still another interesting feature of the HMF model that deserves parallel study and generalization in the  $\alpha - XY$  model. Metastable states have been observed in microcanonical simulations that give rise to anomalous thermodynamics and dynamics. In the range of energy density  $0.5 < U < U_c = 0.75$  states with an initial uniform distribution of  $L_i$ 's (water bag distribution) have a slow relaxation and display a negative specific heat [21][22][29][30]. The average kinetic energy, anomalously relaxes to a value which correspond to a temperature value smaller than the canonical predicted one. The effect is purely microcanonical and was also justified theoretically through the microcanonical solution of HMF model [31]. The velocity distribution of these states



is not Gaussian [8] and anomalous diffusion appears in the form of superdiffusion [20][23][29]. These states are metastable and called *quasi stationary states* because they have a lifetime which increases with  $N$ . The lifetime of these states can be estimated either from the relaxation of temperature to its canonical value or from the crossover of the mean square displacement from the superdiffusive to the normal diffusive behaviour. The two estimates coincide and the lifetime is found to grow linearly with  $N$  [29].

When these states are considered the system then shows different characteristics according to the order of limits in the computation of observables. The idea is presented in Fig. 5 of [14]. If the thermodynamic limit is carried on before temporal average metastable features sussist with their anomalies; on the contrary if the  $N \rightarrow \infty$  limit is taken as the second, normal canonical prediction are valid and no superdiffusion is observed.

We believe these states are present also in the model we presented, eq. (1). Accordingly we simulated the system at an energy density in the above cited range and computed the velocity distribution function at different times, see Fig. 8a, b. Though the numerical distribution is constructed only through average on particles at fixed time and is not therefore a smooth curve, it does not show a relaxation to the Gaussian predicted form (continuous curve)

$$F(L) = \frac{1}{\sqrt{2\pi T}} e^{-L^2/T} \quad (19)$$

The logarithmic scale shows a difference in the tails of the distribution resulting in a different microcanonical temperature (variance of the simulative distribution) smaller than the canonical predicted one (variance of the theoretical distribution). Probably the latter is reached for longer integration times together with the gaussian form for the distribution. The affirmation is currently under verification. We conjecture that Tsallis' generalized thermostatics may help to describe the features these states show.

## 5 Conclusions

In the first part of this paper we have shown that the  $\alpha$ -XY model is canonically equivalent to the HMF model. Through a rescaling by  $\tilde{N}$ , as defined in (12), it is possible to map all thermodynamic functions of the  $\alpha$ -XY model into that of HMF. All  $\alpha$ -models have the same universal canonical thermodynamics, that of the mean field model for  $\alpha = 0$ . In these proceedings a microcanonical solution of the HMF model has been given [31]; a similar solution of the  $\alpha$ -model will complete the proof of this kind of universality.

A dynamical equivalence between the HMF model and the  $\alpha$ -XY model is also suggested by our initial exploration of quasi stationary states in Fig. 8a, b. Let us note that what has been said for the thermodynamic limit of these states in the HMF model should be extended to the corresponding states of the  $\alpha$ -model.

Another kind of universality has been found studying how maximal Lyapunov exponents become zero in the thermodynamic limit in the nonextensive  $\alpha < d$  case. The curve  $\kappa(\alpha/d)$  is universal; the way mixing is reduced by the range of interaction in these  $\alpha$ -models is controlled by the ratio  $\alpha/d$ . Firpo has given the theory of the scaling of  $\lambda_{max}$  with  $N$  for the HMF model [24]. It would

be nice to extend this theory to predict the universal form of the  $\kappa(\alpha/d)$  curve of our Fig. 7. If the reduction of mixing here reported is connected with Tsallis' nonextensive thermodynamics it should be possible to find out a strict relationship between Tsallis' entropic index  $q$  and  $\alpha/d$ ; for  $\alpha/d < 1$  and searching at equilibrium states in the limit  $t \rightarrow \infty$   $N \rightarrow \infty$ , as discussed by Constantino Tsallis in his contribution.

Friendly and wit remarks by Stefano Ruffo have been very useful while we were writing this review paper.

## References

- [1] D. Ruelle. *Statistical Mechanics: rigorous results*. Addison-Wesley, New York (1989).
- [2] G. Gallavotti. *Statistical Mechanics: a short treatise*. Springer, Berlin (1999).
- [3] D. Lynden-Bell. Negative specific Heat in Astronomy, Physics and Chemistry, *Physica A* **263**, 293-304 (1999).
- [4] W. Thirring. Stability of Matter, *Foundations of Physics* **20**, 1103-1110 (1990).
- [5] A very clear and insightful review of the static and dynamic anomalies induced by long-range forces can be found in the introduction of Ruffo's contribution to these proceedings. In order to have extensivity guaranteed the many-body potential energy of a system is required to fulfill two conditions: *stability*, and *tempering* (see again [1] and [2]).
- [6] See also the remarkable contribution by D. H. E. Gross to these proceedings for a purely microcanonical treatment of the thermo-statistics of small non extensive systems, without invoking the thermodynamic limit. Dr. Gross explicitly suggests to go back at pre-Gibbsian times; at Boltzmann's original inspiration. A suggestion to be followed. In our opinion a starting point could be the masterly etymological and conceptual analysis that G. Gallavotti gave of an almost-neglected 1884 Boltzmann's paper (see G. Gallavotti. Ergodicity, ensembles, irreversibility in Boltzmann and beyond, *J. Stat. Phys.* **78**, 1571-1589 (1995)).
- [7] We have found illuminating the paper: M. Antoni, S. Ruffo and A. Torcini. Dynamics and Statistics of Simple Models with Infinite-range Attractive Interaction, preprint cond-mat/9908336.
- [8] V. Latora and A. Rapisarda. Dynamical Quasi-Stationary States in a system with long-range forces, contribution to this conference, preprint cond-mat/0006112.
- [9] C. Anteneodo and C. Tsallis. Breakdown of Exponential Sensitivity to Initial Conditions: Role of the Range of Interactions, *Phys. Rev. Lett.* **80**, 5313-5316 (1998).

- [10] M. E. Fisher and D. Ruelle. The Stability of Many-Particle Systems, *J. Math. Phys.* **7**, 260-270 (1966).  
M. E. Fisher and J. L. Lebowitz. Asymptotic Free Energy of a System with Periodic Boundary Conditions, *Commun. math. Phys.* **19**, 251-272 (1970).
- [11] M. Antoni and S. Ruffo. Clustering and relaxation in Hamiltonian long-range dynamics, *Phys. Rev. E* **52**, 2361-2374 (1995).
- [12] F. Tamarit and C. Anteneodo. Rotators with Long-Range Interactions: Connection with the Mean-Field Approximation, *Phys. Rev. Lett.* **84**, 208-211 (2000).
- [13] The study of Tsallis nonextensivity in magnetic lattice models has also been studied by: S. Cannas and F. Tamarit. Long-range interactions and nonextensivity in ferromagnetic spin models, *Phys. Rev. B* **54**, R12661-R12664 (1996); L.C. Sampaio, M.P. de Albuquerque, and F.S. de Menezes. Nonextensivity and Tsallis statistics in magnetic systems, *Phys. Rev. B* **55**, 5611-5614 (1997).
- [14] C. Tsallis. Entropic nonextensivity: a possible measure of complexity, contribution to this conference.
- [15] The  $N$  behaviour of the quantity  $S$ , eq. (2) can be estimated shifting to the integral  $\int_1^{N^{1/d}} r^{d-1-\alpha} dr$  which gives  $S \sim N^{1-\alpha/d}$ .
- [16] A. Campa, A. Giansanti, and D. Moroni. Canonical solution of a system of long-range interacting rotators on a lattice, *Phys. Rev. E* **62**, 303-306 (2000).
- [17] H. Yoshida. Construction of higher order symplectic integrators, *Phys. Lett. A* **150**, 262-268 (1990).
- [18] Y. Li and S. Teitel. Finite-size scaling study of the three-dimensional classical XY model, *Phys. Rev. B* **40**, 9122-9125 (1989).
- [19] G. Benettin, L. Galgani and J. M. Strelcyn. Kolmogorov entropy and numerical experiments, *Phys. Rev. A* **14**, 2338-2345 (1976).
- [20] V. Latora, A. Rapisarda, and S. Ruffo. Chaos in the Thermodynamic Limit, *Progr. Theor. Phys. Suppl.* **139** (2000) in press, preprint cond-mat/0001010.
- [21] V. Latora, A. Rapisarda, and S. Ruffo. Lyapunov Instability and Finite Size Effects in a System with Long-Range Forces, *Phys. Rev. Lett.* **80**, 692-695 (1998).
- [22] V. Latora, A. Rapisarda, and S. Ruffo. Chaos and Statistical Mechanics in the Hamiltonian Mean Field model, *Physica D* **131**, 38-54 (1999).
- [23] V. Latora, A. Rapisarda, and S. Ruffo. Chaotic dynamics and superdiffusion in a Hamiltonian system with many degrees of freedom, *Physica A* **280**, 81-86 (2000).

- [24] M. C. Firpo. Analytic estimation of the Lyapunov exponent in a mean-field model undergoing a phase transition, *Phys. Rev. E* **57**, 6599-6603 (1998).
- [25] L. Casetti, C. Clementi, and M. Pettini. Riemannian theory of Hamiltonian chaos and Lyapunov exponents, *Phys. Rev. E* **54**, 5969-5984 (1996).
- [26] P. Butera and G. Caravati. Phase transition and Lyapunov characteristic exponents, *Phys. Rev. A* **36**, 962-964 (1987).
- [27] A. Campa, A. Giansanti, D. Moroni, C. Tsallis. Long-range interacting classical systems: universality in mixing weakening, *submitted to Phys. Rev. Lett.*, preprint cond-mat/0007104.
- [28] W. C. Swope, H. C. Andersen, P. H. Berens and K. R. Wilson. A computer simulation method for the calculation of equilibrium constants for the formation of physical clusters of molecules: Application to small water clusters, *J. Chem. Phys.* **76**, 637-649 (1982).
- [29] V. Latora, A. Rapisarda, and S. Ruffo. Superdiffusion and Out-of-Equilibrium Chaotic Dynamics with Many Degrees of Freedoms, *Phys. Rev. Lett.* **83**, 2104-2107 (1999).
- [30] V. Latora and A. Rapisarda. Microscopic dynamics of a phase transition: equilibrium vs out-of-equilibrium regime, preprint nucl-th/0007038.
- [31] M. Antoni, H. Hinrichsen, and S. Ruffo. On the microcanonical solution of a system of fully coupled particles, contribution to this conference, preprint cond-mat/9810048v2.

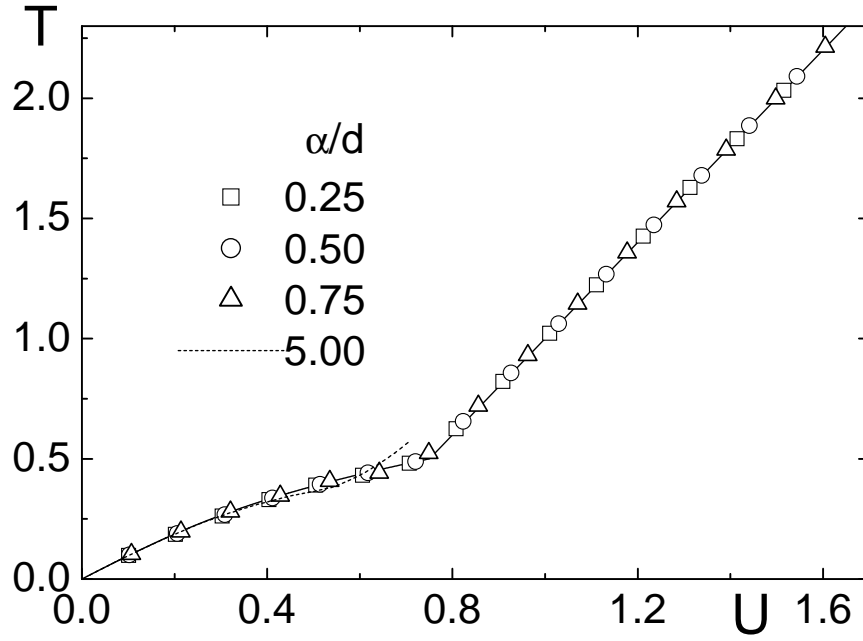


Figure 1: The solid line gives the canonical theoretical caloric curve (temperature  $T$  vs energy density  $U$ ) for model (1) compared with microcanonical simulations of the model on a three-dimensional simple cubic lattice. Three values of  $\alpha$  below  $d$  (symbols) and one value above (dashed line) are shown. Note the qualitative difference between the two cases.

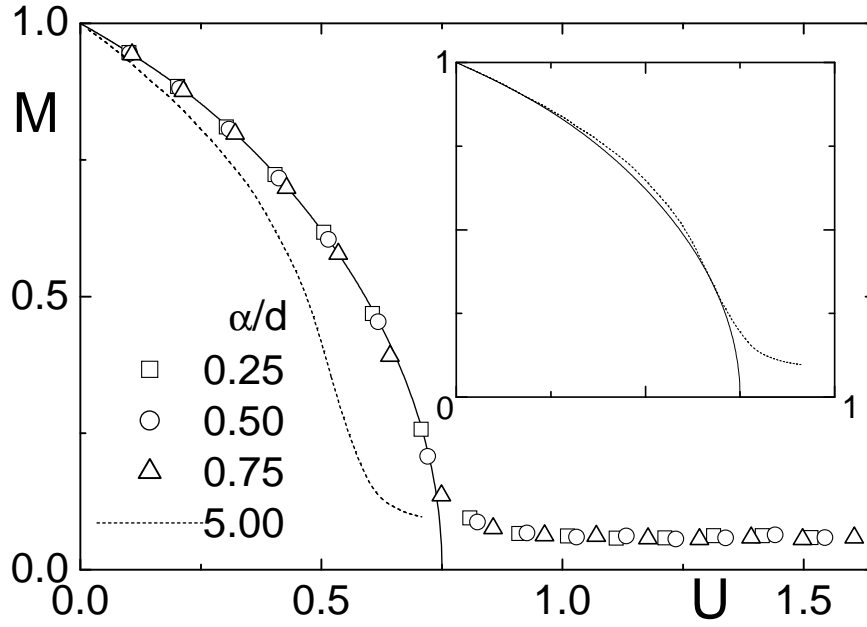


Figure 2: The solid line gives the canonical theoretical magnetization curve (magnetization  $M$  vs energy density  $U$ ) for the system. The simulative points are represented by symbols for the long-range ( $\alpha < d$ ) cases and by the dashed line for the short-range ( $\alpha > d$ ) case. The difference between the long-range and the short-range case is shown in the inset where the impossibility for overlapping through abscissa rescaling is evident because of a different critical exponent.

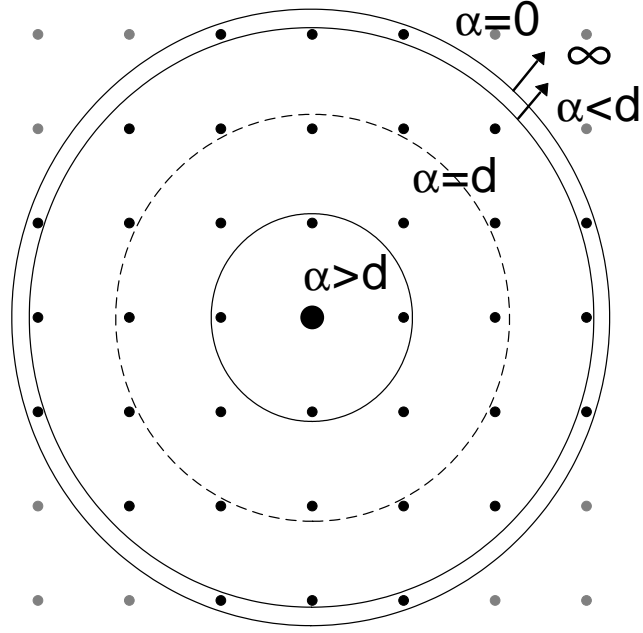


Figure 3: Interaction area: it diverges for  $\alpha < d$ , is finite for  $\alpha > d$ . The long range makes all areas infinite and equal to each other.

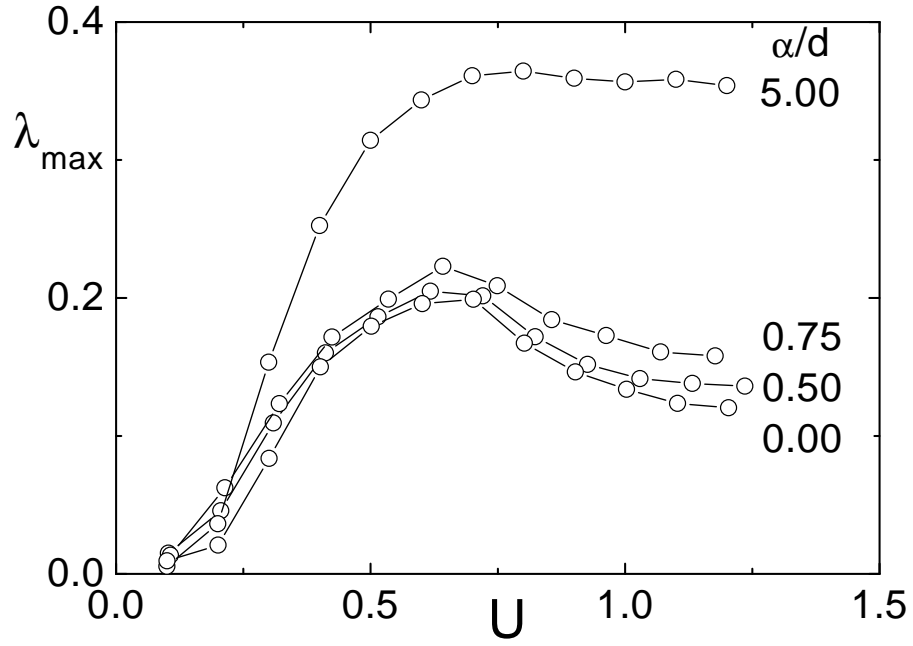


Figure 4: Curves  $\lambda_{\max}(U)$  for  $d = 3$  ( $N = 343 = 7^3$ ) and  $\alpha/d = 0, 0.5, 0.75, 5$ . Note the similarity between the long-range curves for  $\alpha < d$ .

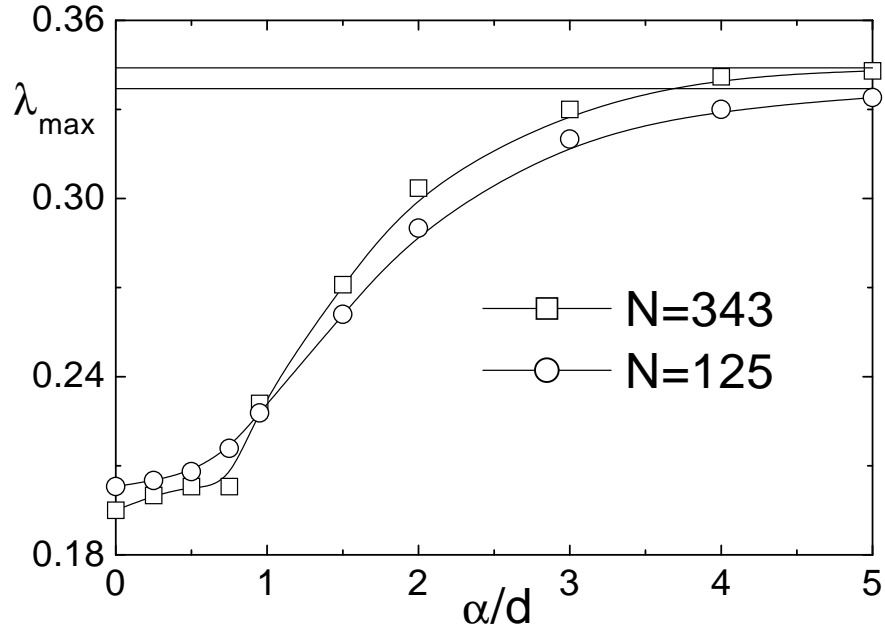


Figure 5:  $\lambda_{\max}(\alpha/d)$  for  $d = 3$ ,  $U = 0.6$ , and  $N = 343 = 7^3$ ,  $125 = 5^3$ . Solid curves are  $B$ -spline interpolations to be used as a guide for the eye. The long-range ( $\alpha < d$ ) points are much closer than the short-range ( $\alpha > d$ ) ones. The horizontal lines are drawn at the simulative values of  $\lambda_{\max}$  found for  $\alpha/d = \infty$  (first neighbour model).



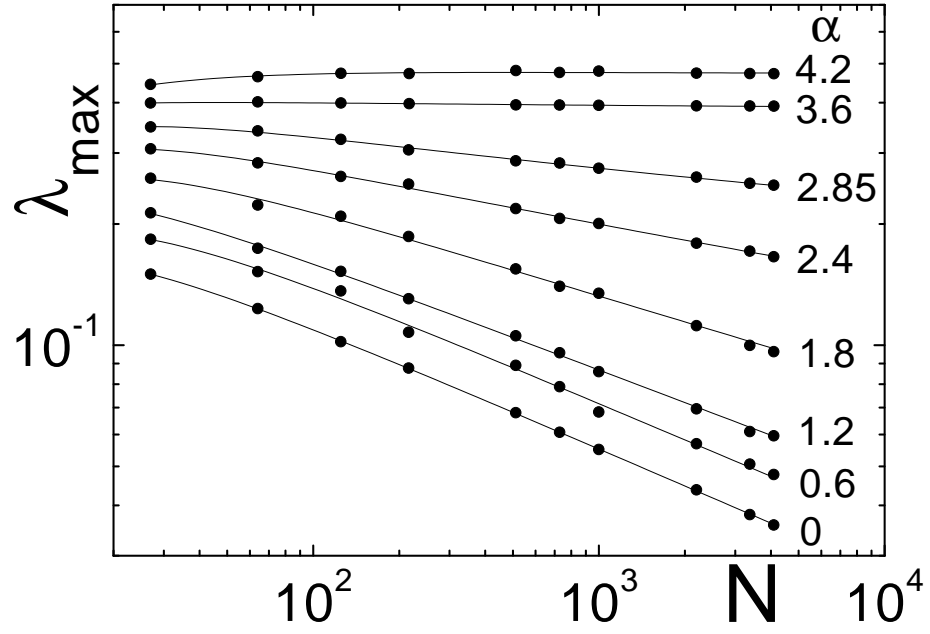


Figure 6:  $\lambda_{max}$  vs  $N$  (log-log plot) for  $d = 3$ ,  $U = 5$  and varying  $\alpha$ . Solid lines are fits with the functional form  $(a - \frac{b}{N})/(\tilde{N})^c$

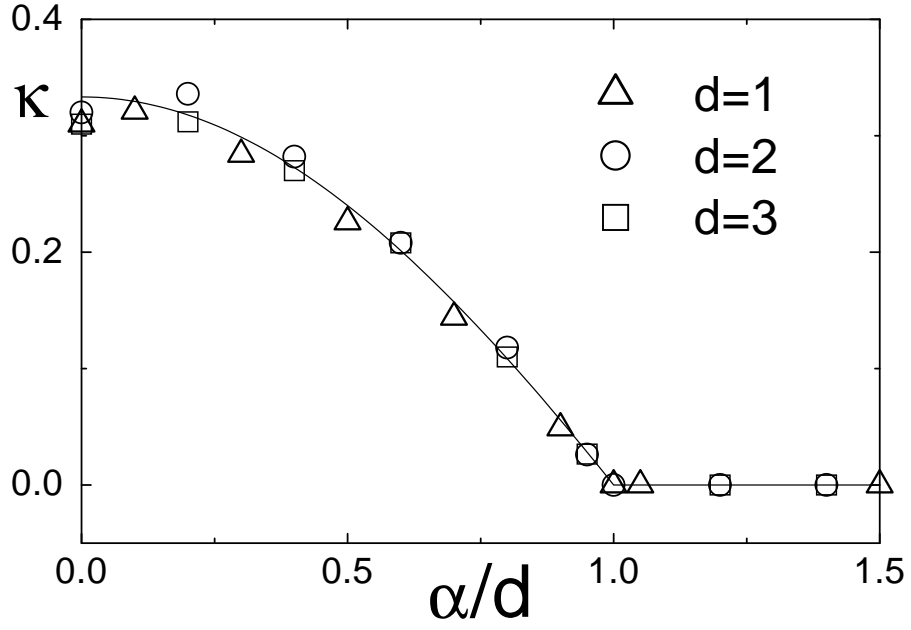


Figure 7: The mixing weakening exponent  $\kappa$  vs  $\alpha/d$  for  $d = 1, 2, 3$  ( $d = 1$ : from [9];  $d = 2, 3$ : from [27]). It describes the asymptotic  $N$  behaviour of the maximal Lyapunov exponent  $\lambda_{max}$  at fixed energy above the critical one, i.e.,  $\lambda_{max} \propto 1/N^\kappa$ . The solid line is a guide to the eye consistent with universality. For  $\alpha = 0$  we have [24]  $\kappa(0) = 1/3$  ( $\forall d$ ). Figure from [27].

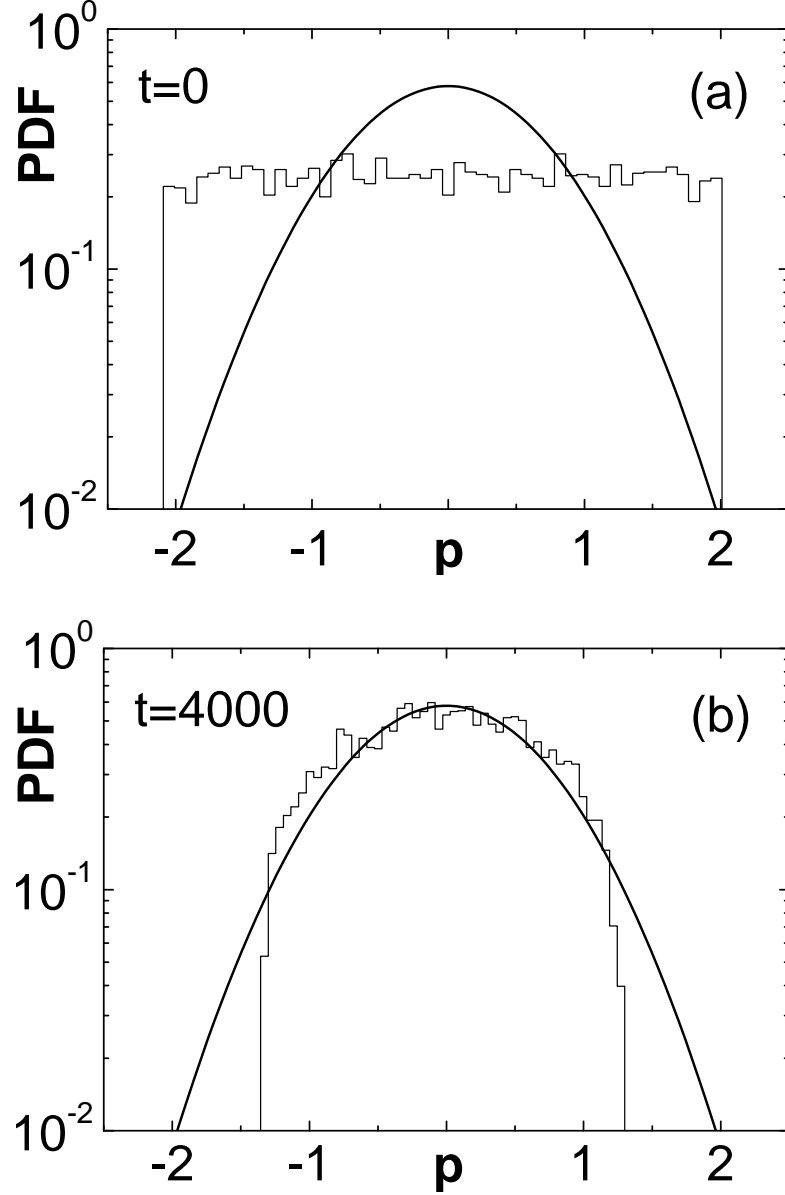


Figure 8: Time evolution of probability distribution function (PDF) for the momentum  $p$  compared with the theoretical canonical one. The graphs refer to a three dimensional simple cubic lattice and  $N = 4096, \alpha = 0.6, U = 0.69$ . Water bag initial ( $t = 0$ ) distribution is shown in (a). Microcanonical velocity distribution at  $t = 4000$  is shown in (b): the microcanonical temperature defined as the variance of this distribution gives the value  $T = 0.39$ . continuous curves are the canonical distribution computed for  $T = 0.4757$  (see eq. (19)), corresponding to  $U = 0.69$  in the canonical caloric curve, see Fig. 1.